Title: Mesothelin overexpression promotes mesothelioma cell invasion and MMP-9 secretion in an orthotopic mouse model and in epithelioid pleural mesothelioma patients

Authors: *Elliot L. Servais MD[1,2], *Christos Colovos MD PhD[1,2], Luis Rodriguez MS[1,2], Adam J. Bograd MD[1,2], Jun-ichi Nitadori MD PhD[1], Camelia Sima, MD, MS[3], Valerie W. Rusch MD[1], Michel Sadelain MD PhD[2,4], Prasad S. Adusumilli MD, FACS[1,2]

* (ELS and CC contributed equally to this manuscript)

Division of Thoracic Surgery[1], Center for Cell Engineering[2], Departments of Epidemiology & Biostatistics[3], and Medicine[4], Memorial Sloan-Kettering Cancer Center, New York, NY

Running Title: Mesothelin promotes invasion in mesothelioma

Keywords: Mesothelin, mesothelioma, matrix metalloproteinase, tumor invasion, locoregional aggressiveness

Financial Support: This work was supported in part by PR101053 Department of Defense Research Grant; Mesothelioma Applied Research Foundation (MARF) Grant in memory of Lance S. Ruble; William H. Goodwin and Alice Goodwin, the Commonwealth Foundation for Cancer Research, the Experimental Therapeutics Center of Memorial Sloan-Kettering Cancer Center; American Association for Thoracic Surgery (AATS)-Third Edward D. Churchill Research Scholarship; IASLC – International Association for the Study of Lung Cancer Young Investigator Award; National Lung Cancer Partnership/LUNGevity Foundation Research Grant; Stony Wold-Herbert Fund; New York State Empire Clinical Research Investigator Program (ECRIP); and U54CA137788/U54CA132378 from the National Cancer Institute.

Corresponding Author
Prasad S. Adusumilli, MD, FACS
Division of Thoracic Surgery
Memorial Sloan-Kettering Cancer Center
1275 York Ave.
New York, NY, 10065
Tel: 212-639-8093
Fax: 646-422-2340
Email: adusumip@mskcc.org

Conflicts of Interest: The authors declare no conflict of interest.
Word Count : 4523
Total Number of Figures and Tables : 6

Abstract

Purpose: Mesothelin (MSLN) is a tumor-associated antigen, being investigated as a biomarker and therapeutic target in malignant pleural mesothelioma (MPM). The biological function of MSLN overexpression in MPM is unknown. We hypothesized that MSLN may promote tumor invasion in MPM, a tumor characterized primarily by regional aggressiveness and rare distant metastases.

Experimental Design: Human and murine MPM cells with MSLN forced expression and shRNA knockdown were examined for proliferation, invasion, and matrix metalloproteinase (MMP) secretion. The influence of MSLN overexpression on MPM cell invasion was assessed in an orthotopic mouse model and in patient samples.

Results: MSLN expression promotes MPM cell invasion and MMP secretion in both human and murine MPM cells. In an orthotopic MPM mouse model characterized by our laboratory, MPM cells with MSLN overexpression preferentially localized to the tumor invading edge, co-localized with MMP-9 expression, and promoted decreased survival without an increase in tumor burden progression. In a tissue microarray from epithelioid MPM patients (n=139, 729 cores), MSLN overexpression correlated with higher MMP-9 expression at individual core level. Among stage III MPM patients (n=72), high MSLN expression was observed in 26% of T2 tumors and 51% of T3 tumors.

Conclusions: Our data provide evidence elucidating a biological role for MSLN as a factor promoting tumor invasion and MMP-9 expression in MSLN-expressing MPM. As regional invasion is the characteristic feature in MSLN-expressing solid cancers (MPM, pancreas, and ovarian), our observations add rationale to studies investigating MSLN as a therapeutic target.

Translational relevance

Mesothelin (MSLN) is a cancer-associated antigen overexpressed in malignant pleural mesothelioma (MPM) and other regionally invasive malignancies. We hypothesized that MSLN expression promotes MPM cell invasion. In human and murine MPM cells with MSLN overexpression and knockdown, we show that MSLN promotes MPM cell invasion. In an orthotopic MPM mouse model characterized by our laboratory, we demonstrate that MSLN overexpressing MPM cells preferentially localize to the tumor invading edge and decrease survival without an increase in tumor burden progression. Both *in vitro* and *in vivo,* and in MPM patient samples, we demonstrate an association between MSLN overexpression, tumor invasion and matrix metalloproteinases (MMPs), a family of enzymes that facilitate tumor cell invasion and known to be upregulated in MPM. As regional invasion is a characteristic feature in MSLN-expressing solid cancers (MPM, pancreas, and ovarian), these findings add support for studies investigating MSLN as a therapeutic target.

Introduction

Mesothelin (MSLN) is a 40-kDa glycoprotein overexpressed in mesothelioma, pancreatic and ovarian cancers – malignancies characterized by regionally aggressive phenotypes and poor prognosis(1-3). Although MSLN is being investigated as a tumor biomarker and therapeutic target in MPM, the biological role of MSLN remains unexplored(4-9).

MSLN is highly expressed in epithelioid MPM, the most common MPM subtype constituting 80% of patients. Only 3% of epithelioid MPM patients demonstrated distant metastases in multiple series published by our group(10-12). Despite an absence of distant metastases, a majority of epithelioid MPM patients are not eligible for surgical resection due to advanced T-stage (T3 tumors are unresectable due to local invasion into the endothoracic fascia, mediastinal fat, chest wall or pericardium compared to T2 tumors without invasion)(13-15). Matrix metalloproteinases (MMPs), a family of endopeptidases capable of degrading extracellular matrix, have been shown to be elevated in MPM and are known to increase invasive potential in MPM cells(16). Furthermore, asbestos exposure, a causative agent in MPM, is known to upregulate both MSLN and MMP-9 secretion in experimental models of asbestosis(17).

In this study, we explored the role of MSLN in tumor invasion and its relationship to MMP-9 secretion using human and murine mesothelioma cells both *in vitro* and *in vivo* as well as in clinical specimens from epithelioid MPM patients, known to overexpress MSLN. We demonstrate for the first time that MSLN promotes MMP-9 expression as

well as tumor invasion shown by MSLN forced overexpression and confirmed by shRNA knockdown experiments in mesothelioma cells. To further elucidate MSLN biology in an appropriate tumor microenvironment, we developed and characterized an orthotopic MPM mouse model. With this model, we demonstrate that MSLN-expressing MPM cells are invasive, express MMP-9 on the invasive tumor edge, and decrease overall survival independent of tumor cell proliferation or metastasis. Furthermore, our clinical observations from a large cohort of epithelioid MPM patients demonstrate that MSLN expression correlates with MMP-9 expression. The results reported herein provide evidence that MSLN also plays an important role in MPM biology and suggest the MMP pathway as a mediator of invasiveness in MSLN-expressing MPM.

Materials and Methods

Cell lines and culture

MSTO-211H (human pleural mesothelioma) and AB12 (murine mesothelioma line) were obtained from American Type Culture Collection and CellBank Australia, respectively. MSTO-211H cells were maintained in RPMI-1640 media and AB12 cells in DMEM in a 5% CO_2 humidified incubator at 37°C – all media was supplemented with 10% fetal bovine serum(FBS), 100 units/mL penicillin, and 100 ug/mL streptomycin.

Establishment of stably transduced cell lines

Green fluorescent protein-firefly luciferase fusion was cloned into a SFG retroviral vector and transfected into H29 cells with calcium phosphate. MSTO-211H were plated in 24-well plates 24 hours prior to transduction. Filtered virus was added to cells

permeablized with 8μg/mL polybrene(Sigma-Aldrich, MO) and reinfected 24 hours later. The human MSLN-variant 1 was isolated from a human ovarian cancer cell line (OVCAR-3). RT-PCR synthesis of full-length cDNA of human MSLN was performed using SuperScript™ III One-Step RT-PCR System with Platinum® *Taq* High Fidelity Kit. Plasmid DNA was isolated, subcloned into a SFG retroviral vector, confirmed by sequencing, and used to stably transduce MSLN. For experiments comparing MSLN-transduced cells to MSLN-negative cells, transduction control was performed with a GFP-Luciferase vector. For all experiments, a stably-transduced population of cells was used with confirmation of unchanged MSLN expression by flow cytometery and western blot analysis.

Mesothelin knockdown with MSLN specific shRNA

To obtain a stable cell line with decreased murine MSLN expression, three predesigned siRNA oligonucleotides and complementary murine MSLN shRNA sequences were obtained(Ambion, TX), ligated into the pSilencer 2.1-U6 hygro plasmid(Ambion, TX), and transfected into the AB12 cell line with calcium phosphate. After 2 week selection with 500μg/ml hygromycin(Invitrogen, CA) the AB12 cell line demonstrating greatest murine MSLN silencing by flow cytometry, qPCR analysis, and western blot was selected for subsequent experiments and is denoted by AB12shRNA. AB12 cells were also transfected with scramble shRNA as a control.

Flow Cytometry

Fluorescence activated cell sorting(FACS) was performed following retroviral transductions using a FACSAria(BD Biosciences) cytometer to sort for a pool of highly-transduced cells. Human MSLN expression was detected using a PE-conjugated or APC-conjugated anti-human MSLN rat IgG_{2a}(R&D systems, MN). Murine MSLN expression was detected with an anti-mouse MSLN rat IgG_{2a} primary antibody(MBL, Japan). Subsequent flow cytometry for GFP and MSLN expression analysis was performed on either FACSCaliber or LSRII cytometers(BD Biosciences) and analyzed using FlowJo(TreeStar) analysis software.

Cell proliferation assays

MSTO-211H cells with or without MSLN expression were plated in 6-well tissue culture plates at a density of $1x10^5$ cells/3 mL/well and were counted on days 1, 2, 4, and 6. At each time point cells were counted in triplicate using trypan exclusion after brief trypsinization. Cell number versus time was plotted for each cell line and compared at time points using a Student's T-test.

Invasion and migration assays

BD BioCoat™ Matrigel™ Invasion Chamber(BD Biosciences) assays were performed in 24-well plates using polyethylene terephthalate inserts(8μm pores) without matrigel (for migration) and with matrigel coating (for invasion assays). Cells were seeded in the upper well of the chamber ($5x10^4$ - $1x10^5$) in 0.5 mL RPMI-1640 without FBS and 0.75 mL RPMI-1640 with 10% FBS in the bottom chamber. Migration was assessed at 12

hours and invasion at 24 hours for MSTO-211H. For AB12 cells, migration was assessed at 6 hours and invasion at 20 hours. Nonmigrating or noninvading cells were removed from the upper membrane surface of the insert using a cotton swab. The insert membrane was fixed and stained using the Diff-Quik™ staining system and mounted on glass slides. Stained cells were counted in 10 high-power fields in predetermined areas of the membrane.

Orthotopic pleural mesothelioma animal model

To develop the orthotopic mouse model of pleural mesothelioma, female SCID/beige or BALB/c mice(Taconic, NY) at 6-10 weeks of age were utilized. All procedures were performed under approved Institutional Animal Care and Use Committee protocols. Mice were anesthetized using inhaled isoflurane and oxygen. Direct intrapleural injection of $1x10^5$ tumor cells in 200μL serum-free media via a right thoracic incision was performed to establish orthotopic MPM tumors as previously described(18-21). For experiments to establish heterogeneously MSLN expressing tumors, mice were inoculated by direct pleural injection with a mixture of $1x10^5$ MSTO-211H expressing and deficient in MSLN.

Histology and immunostaining

Histopathological evaluation of tumors was performed following hematoxylin and eosin staining of paraffin-embedded, 4% paraformaldehyde fixed tissue samples. For angiogenesis, CD34 rat monoclonal antibody (5ug/ml, eBioscience) was incubated for 7 hours, followed by 16 minutes with (1:200) biotinylated rabbit anti-rat IgG (Vector Labs,

Cat. #BA-4000). Rat IgG_{2a} (5ug/ml) was used as an appropriate isotype negative control. For lymphangiogenesis, goat polyclonal LYVE-1 antibody (1µg/ml; R&D Systems) was incubated for 3 hours, followed by 60 minutes with biotinylated rabbit anti-goat IgG (ABC kit from Vector labs). The protocols for immunofluorescence detection using Tyramide-Alexa Fluor 488(Invitrogen) or Tyramide-Alexa Fluor 568(Invitrogen) for CD34 and LYVE-1, respectively, were established and performed at the MSKCC Molecular Cytology Core Facility using a Discovery XT automatic processor (Ventana Medical Systems). Immunohistochemistry for human MSLN was performed with a mouse anti-human MSLN IgG(1:100, Vector Labs, CA) using the Ventana platform. Immunohistochemistry for MMP-9 was performed by Premier Laboratories(Boulder, CO) using polyclonal rabbit anti-human MMP-9(Dako, CA). Immunohistochemistry for MMP-7 was performed utilizing a mouse IgG_{2b} anti-human MMP-7 clone ID2 (abcam, Cambridge, MA) in a 1:100 dilution. Placenta with cytoplasmic staining in the villi was used as the MMP-7 positive control.

Quantitative bioluminescence imaging

In vitro standardization was performed using GFP-Firefly Luciferase expressing MSTO-211H cells with and without MSLN expression. Serially diluted cells were plated in 96-well tissue culture plates ($1.6x10^6$ to $2.5x10^4$ cells/100µL/well). Twenty minutes after the addition of 100µL D-Luciferin (15mg/mL; Caliper Lifesciences, MA), plates were imaged using the Xenogen IVIS 100 Imaging System(Caliper Lifesciences). Cell number versus total BLI flux(photon/s) was evaluated by Pearson's correlation.

In vivo BLI in tumor-bearing mice was performed using a single intraperitoneal dose of 150mg/kg D-Luciferin. Mice were imaged with the Xenogen IVIS 100 Imaging System 20 minutes following D-Luciferin injection. Images were acquired for 5-30 seconds depending on signal strength. BLI data were analyzed using Living Image 2.60 software and BLI signal reported as total flux(photons/s).

Magnetic resonance imaging

Magnetic resonance imaging(MRI) was performed in a Bruker 4.7T USR scanner(Bruker Biospin Inc., Ettlingen, Germany) equipped with a 400 mT/m gradient coil and a 32 mm ID custom build birdcage resonator. Thoracic axial MRI images were acquired using a RARE fast spin-echo sequence (repetition time(TR)=1.7s, echo time(TE)=40 ms, and 12 averages). The slice thickness was 0.7 mm and the in-plane image resolution was 117 x 156 mm. Image acquisition was triggered by animal respiration and tumor volumes (mm^3) were calculated from tracing tumor boundaries in each slice using Bruker ParaVision Xtip software(Bruker Biospin Inc., Ettlingen, Germany).

Gene expression analysis

Gene expression profiles were compared between MSLN-expressing and non-expressing MSTO-211H cells. Cell pellets were collected in triplicate and snap frozen from 3 separate plates for each cell line. The Genomics Core Laboratory at MSKCC collected, processed, and hybridized RNA samples to Illumina Humanref-6 BeadChips. Using Bioconductor package LIMMA, sample probesets were normalized to control

probesets to minimize inter-beadchip variability. Individual gene expression was screened for significance using a false discovery rate (FDR) threshold of <0.05 and a fold change threshold of 1.5. Gene set enrichment analysis (GSEA)(22) was performed to determine biological pathways related to MSLN overexpression.

Matrix metalloproteinase assays

MMP secretion by tumor cells *in vitro* was quantified by multiplex bead assays (Millipore, MA) for MMP-1, MMP-2, MMP-7, and MMP-9 on a Luminex 100 xMAP with internal quality control standards for each analyate. $1x10^5$ cells in 1mL media were plated in 24-well tissue culture plates and allowed to grow for 24 hours, media was then removed, washed with PBS, and media replaced with 0.5mL RPMI-1640 without FBS. Cell supernatant MMP-9 secretion was quantified by multiplex bead assay for MMP-9 (Millipore, MA). Supernatant was collected 12, 24, and 36 hours after media exchange and stored at -80°C until analyzed.

Epithelioid MPM tissue microarray and immunohistochemistry

Patients diagnosed with epithelioid MPM between 1989 and 2009 at Memorial Sloan-Kettering Cancer Center were included. For each of the 139 patients with available specimens, all H&E slides (median 9, range 1-43) were reviewed. Representative blocks were selected to construct a tissue microarray (TMA) by taking nine representative cores(0.6 mm) from each patient tumor block and ensuring at least six complete tumor cores. Five-µm sections were cut from the TMA and stained by specific antibodies (MSLN:Vector, 1:200 dilution; MMP-9:Oncogene Science, 1:200 dilution).

Grading of MSLN and MMP-9 intensity was performed on separate occasions by a pathologist who was blinded to the clinical data as follows: 0(absent stain), 1(weak expression), 2(moderate expression), and 3(strong expression). The distribution of MSLN-positive tumor cells from all tumor cells found in a single core was graded as 0(absent), 1(1-50%), and 2(51-100%). The sum of the MSLN stain intensity and distribution grades was used to determine a total MSLN score ranging from 0 to 5 at the core level. MSLN score for each patient was then determined using the average of all tumor cores.

We examined the correlation between MMP-9 and MSLN expression using Mantel-Haenszel correlation statistic. The p-values were adjusted through bootstrap to account for the fact that each of the 139 patients can contribute with more than one core to the analysis, leading to a total of 721 cores. The correlation between increasing MSLN expression and T-stage was determined using the Fisher's exact test.

Results

Mesothelin expression promotes invasion and migration in vitro independent of tumor cell proliferation

We initially investigated the effect of MSLN overexpression on MPM by comparing MSTO-211H cells without MSLN expression to those stably transduced to overexpress MSLN(Fig. 1A) and AB12 cells with natural MSLN expression or knockdown(Fig. 1B). We noted no morphological differences in cultured cells overexpressing MSLN and cell-counting assays demonstrated no effect of MSLN expression on MSTO-211H

proliferation (Fig. 1C). Similarly, we observed no differences in morphology or log-phase growth rates between AB12 cells transfected with control scramble shRNA or MSLN-specific shRNA (data not shown). In order to examine if MSLN expression promoted changes in MSTO-211H proliferation during periods of cellular stress, experiments were repeated with serum-starved(2% FCS) media; no differences were observed (data not shown). Since local invasion is the characteristic clinical feature of mesothelioma, we evaluated *in vitro* cell migration and invasion using a standard Boyden chamber assay. MSLN overexpression in MSTO-211H significantly increased cell migration(2.56-fold, $p<0.001$) and invasion(1.54-fold, $p<0.001$) compared to non-MSLN expressing MPM cells (Fig. 1D & 1E (left panel)). To confirm our observations of MSLN influence on invasion, we next examined the effect of MSLN-knockdown in the AB12 cell line that natively expresses MSLN(Fig. 1B). Decreased MSLN expression resulted in decreased migration(2.14-fold, $p<0.001$) and invasion (2.35-fold, $p<0.0001$)(Fig. 1E (right panel)). These results demonstrate that MSLN overexpression promotes invasion in MPM cells.

Development and characterization of a clinically relevant orthotopic mouse model of MPM to investigate mesothelin biology

Having noticed that MSLN overexpression promotes MPM invasion and migration *in vitro*, we next sought to investigate the biology of MSLN within an appropriate tumor microenvironment. In order to evaluate local pleural and chest wall invasion, an important clinical factor in the progression of MPM, which cannot be fully simulated in subcutaneous or intraperitoneal mouse models, we developed an orthotopic mouse model by directly inoculating MPM cells into the pleural space(18, 20, 23, 24).

Resultant tumors mimicked human MPM as demonstrated by: (a) gross pleural and mediastinal tumor distribution seen on necropsy and magnetic resonance imaging (MRI) (Fig. 2A); (b) histology demonstrating tumors growing along visceral and parietal pleural surfaces, frequent chest wall and diaphragmatic invasion, and rare lung invasion (Fig. 2B); (c) frequent metastases to mediastinal lymph nodes confirmed by histology (Fig. 2C) without distant metastases; (d) retention of characteristic MPM tumor markers including WT-1, Calretinin, and MSLN even at late stages of disease while TTF-1, a marker of lung adenocarcinoma, remained negative (Fig. 2D); and (e) extensive neo-lymphangiogenesis throughout the MPM tumor specimens by CD34 and LYVE-1 immunofluorescence for angio- and lymphangiogenesis, respectively (Fig. 2E) (MPM is known to be a well vascularized tumor with high levels of VEGF secretion (25, 26)). These findings not only confirm that our orthotopic pleural mesothelioma mouse model resembles human MPM, but also provides an appropriate *in vivo* tumor microenvironment to investigate MPM tumor cell invasion.

Quantitative bioimaging monitors the effect of mesothelin on tumor progression in vivo

Using our orthotopic MPM mouse model, we first sought to evaluate whether MSLN imparts a growth advantage *in vivo*. Unlike subcutaneous flank tumors, which are easily accessible for serial monitoring, evaluating the effect of MSLN expression on pleural tumors required an accurate noninvasive method to serially evaluate tumor burden and progression. To do so, we validated bioluminescencent imaging (BLI) as a quantitative modality to assess tumors in the pleural model. First we performed an *in vitro* BLI

standardization with MSLN-expressing and non-expressing MPM cells stably transduced express a GFP-firefly luciferase fusion gene (Fig. 3A). Our results demonstrated that BLI signal correlated with number of cells for both MSLN-negative (Pearson r = 0.99, $p<0.0001$) and positive (Pearson r = 0.99, $p<0.0001$) cell lines(Fig. 3B). We next validated BLI as an accurate method to monitor tumor progression within the orthotopic MPM mouse model by serially comparing BLI signal to MRI tumor volume averaging, the gold standard for tumor volume assessment(27). BLI signal from the engrafted pleural tumors correlated with MRI tumor volume over a wide range of tumor burdens (r = 0.86, $p<0.0001$; Fig. 3C and D). Thus, this orthotopic MPM mouse model allows for quantifying tumor burden and monitoring tumor progression in the pleural tumor microenvironment (28).

Mesothelin expression promotes tumor invasion in vivo and decreases survival without affecting tumor proliferation

Mice inoculated with equivalent intrapleural MSLN-expressing and non-expressing MPM cells were compared for *in vivo* tumor progression. Serial BLI was used to monitor tumors in mice and revealed no differences in tumor burden between tumors with or without MSLN expression at any point in disease progression (Fig. 4A). Despite equivalent tumor progression rates and tumor burden, mice with MSLN-expressing MPM experienced significantly decreased survival compared to mice with MSLN-negative tumors (29 vs. 37 days, $p=0.001$; Fig. 4B). These results of decreased survival with MSLN expression were reproduced in our syngeneic orthotopic MPM model using BALB/c mice with murine AB12 MPM cells. Mice inoculated with AB12 wild type

(MSLN-expressing) tumors had a median survival of 30 days compared to AB12 shRNA (MSLN-knockdown), which survived the 60-day study period ($p<0.001$). We further evaluated AB12 survival by transducing MSLN-expressing AB12 cells with mouse MSLN vector to express MSLN at even higher levels (AB12 M). We observed decreased survival of mice inoculated with these high MSLN expressing AB12 cells compared to AB12 wild-type cells (24 vs 30 days, $p=0.005$; Supplemental Figure 1).

Systematic histologic evaluation of necropsy specimens demonstrated MSLN-expressing tumors to have qualitatively increased local tumor invasion of chest wall, diaphragm, and mediastinal structures as compared to tumors without MSLN. To further investigate the association between MSLN expression and local tumor invasion *in vivo*, we evaluated mice with orthotopic MPM tumors heterogeneously expressing MSLN. Heterogeneously expressing tumors were established by inoculating mice with a mixture of MSLN-expressing and MSLN-deficient MSTO-211H cells. These tumors uniformly demonstrated clustering of MSLN expression at the advancing (invading) edge as determined by MSLN IHC (Fig. 4C and D upper panel).

Mesothelin expression promotes MMP secretion, which co-localizes at the invading tumor edge

Having observed MSLN expression at the invasive edge of MPM tumors, we next investigated if pathways known to cause tumor invasion were upgregulated in MPM cells overexpressing MSLN. Gene set enrichment analysis (GSEA)(22) of gene array data comparing human MPM cells (MSTO-211H) with or without MSLN expression

demonstrated that MSLN expression increased the expression of genes known to regulate MMP secretion ("SA-MMP-cytokine connection"; hypergeometric $p<0.001$) (Supplemental Table 1). To investigate these findings, we evaluated MMP secretion in cultured human MSTO-211H and murine AB-12 MPM cells. Using multiplex bead assays for human and murine MMPs, we found that MSLN-overexpressing MSTO-211H cells produced significantly increased MMP-1, 2, 7, and 9 compared to MSLN-deficient MPM cells ($p<0.01$, Fig. 5A). To confirm that MSLN expression has a direct relationship to MMP secretion, we examined the effect of MSLN knockdown by shRNA using the MSLN-expressing murine MPM cell line AB12; decreased MSLN expression was confirmed by flow cytometry (Fig. 1B) and qPCR (relative-fold MSLN expression 0.483 ± 0.29). We found that cell supernatant secretion of MMP-9 was significantly decreased following MSLN knockdown in the AB12 cell line ($p<0.0001$, Fig. 5B).

We then evaluated expression of MMP-9 in MPM tumors *in vivo*. We performed IHC for MMP-9 on heterogeneously MSLN-expressing tumors and found increased intensity of MMP-9 staining at the invasive edge co-localizing with MSLN staining compared to the baseline level of MMP-9 staining of non-MSLN expressing cells (Fig. 4D lower panel). These results suggest an association between MMP-9 and MSLN expression *in vivo*.

Mesothelin is overexpressed in 90% of epithelioid MPM patients

As MSLN IHC is not routinely performed in MPM patients, the only MSLN expression data available to date is from small case series (33–49 patients) comprised of varying histological subtypes(29, 30). Therefore, we first evaluated MSLN expression in a large

uniform cohort of epithelioid MPM patients (n=139). MSLN is overexpressed in 90% of epithelioid MPM patients (score 1-5), with strong expression present in 29% of epithelioid MPM patients (score 4-5) (Fig. 6A).

Mesothelin overexpression is associated with high MMP-9 expression in human epithelioid MPM specimens

To determine the relationship between MSLN and MMP-9 expression in human tumor samples, a tissue microarray (6 tumor cores/patient) derived from 139 surgically resected epithelioid MPM tumors(Supplemental Table 2) was examined by IHC(Fig 6A). We detected a strong correlation between MMP-9 expression and MSLN intensity at individual core level – observing increased levels of MMP-9 expression with increasing MSLN expression(Fig. 6B, $p<0.001$). These clinical findings support our preclinical observations associating MSLN expression with increased MMP levels.

Mesothelin intensity and distribution in epithelioid MPM patients

We examined MSLN expression score (sum of intensity and distribution) in stage III epithelioid MPM patients. To avoid confounding effects due to heterogeneous clinical stages and neo-adjuvant therapy, we selected a uniform cohort of 72 stage III patients with no prior therapy (T1=1 (excluded), T2=17 and T3=54 patients). In this cohort, a high MSLN score (4-5) is observed in 26% vs. 51% for T2 and T3 patients, respectively (Fig. 6C, p=0.05). These data are notable since increasing T-stage represents an important clinical distinction of tumor invasion.

Discussion

Tumors that are known to express MSLN including MPM, pancreatic, and serous ovarian cancers are characterized by locoregional aggressiveness(31). Local tumor invasion is the primary cause of morbidity in patients with MPM and the factor most often preventing tumor resectability(11, 14). The majority of studies in MPM and other regionally aggressive malignancies have focused on MSLN as a tumor biomarker(8, 9) and therapeutic target, while none have evaluated the influence of MSLN on tumor biology. Our study provides evidence demonstrating for the first time a correlation between MSLN and MMP expression as well as regional tumor aggressiveness and invasion in MPM cells, in an orthotopic MPM model, and in epithelioid MPM patients

It is well documented that MMP-mediated degradation of extracellular matrix proteins facilitates cancer cell migration and invasion(32, 33). MMPs have been implicated in the tumor progression of several cancers including breast(34, 35), pancreatic(36), lung(37), ovarian(38), and mesothelioma (39, 40). In a recent publication, Chang et al. demonstrate an associated between MMP-7 and MSLN expression in ovarian cancer using murine cell lines and human tumor specimens(41). In this study, we have shown that MSLN overexpression increases tumor cell MMP secretion, whereas shRNA knockdown of MSLN decreases MMP secretion in mesothelioma(Fig. 2A and B; Fig. 3). These data provide evidence that MSLN promotes MMP secretion contributing to tumor aggressiveness. A recent report further highlights the role of MMP-9-mediated invasion in MPM and the beneficial therapeutic efficacy of suppressing MMP-9 expression(42). In addition to MMP-9, we have observed increased *in vitro* secretion of MMP 1, 2, and 7

with MSLN overexpression – consistent with published observations that in promoting cancer cell invasion MMPs can influence each other directly(41, 43). In an orthotopic MPM mouse model, we showed that MSLN and MMP-9 co-localize along the invasive edge of pleural tumor nodules. Although we report for the first time that MSLN is expressed along the invading tumor edge in MPM, other investigators have reported similar observations in rats following exposure to multi-wall carbon nanotubes, which are hypothesized to cause MPM strengthening our observation(44). Furthermore, in colorectal cancer, >50% of patient specimens demonstrated MSLN expression along the invading edge of tumors(45). These data correlate with clinical MPM tumor specimens where we have demonstrated an association between MSLN and MMP-9 expression. It is notable that, in contrast to data reported for ovarian cancer (41), we found no correlation in human MPM tumor specimens between MMP-7 and either MSLN expression or tumor stage (data not shown). Our data suggest that while secretion of multiple MMPs is increased in association with MSLN *in vitro*, MMP-9 plays a predominant role in the *in vivo* human MPM tumor. The results reported herein highlight MMP-9 as a potential pathway for MSLN-mediated MPM invasiveness.

MSLN is a glycophosphoinositol (GPI)-anchored cell-surface protein, for which signal transduction depends upon associating with accessory proteins. GPI-anchored proteins such as T-cadherin can traduce signals that modulate cell migration and invasion by mechanisms mediated through direct interactions with integrin-linked kinase(46) and integrin β3(47). Data from our gene array studies show an association between integrin β4 and MSLN overexpression in MPM (Supplemental Table 1). We have confirmed the

expression of integrin β4 in MSLN overexpressing MPM cells by flow cytometry (Supplemental Figure 2). Integrin β4 is expressed by epithelioid MPM (48), and published literature implicates integrin β4 expression with tumor cell migration, invasion, and MMP expression(49). Further studies to better define the association between MSLN and integrin β4 may ultimately help elucidate this pathway's relationship to MPM tumor cell migration, invasion, and MMP expression.

Review of the literature reveals other putative mechanisms for MSLN's influence on tumor phenotype besides the association with MMP expression that we have demonstrated. Functionally, investigators have shown high-affinity binding between MSLN and CA-125 present on mesothelial cells(50) – an interaction thought to contribute to peritoneal migration of ovarian cancer. Uehara and colleagues (51) have found MSLN overexpression to promote anchorage-independent growth and resistance to anoikis in association with suppression of pro-apoptotic Bim. Chang *et al*(52) have implicated the PI3K pathway in MSLN-associated anti-apoptosis. Perturbations in Wnt1/β-catenin or Ras pathways lead to the expression of MSLN in mammary(53) and pancreatic adenocarcinomas(54). Overexpression of Wnt1 in colorectal cancer cells, which is also often constitutively activated in mesothelioma, ovarian, and pancreatic cancers, was associated with MSLN expression(45). However, these mechanisms neither explain nor provide a pathway for the specific observation of MSLN-associated local tumor invasion, a clinically important characteristic of MSLN-expressing cancers.

Tumor invasion has typically been studied using the Boyden chamber and scratch assays *in vitro*. We have established a novel orthotopic MPM mouse model wherein tumor invasion into diaphragm, mediastinal fat, and pericardium mimic human MPM and have demonstrated that MSLN overexpressing cells localized to the invading edge. Furthermore, to demonstrate that MSLN is indeed associated with invasion, we have utilized a uniform cohort of stage III epithelioid MPM patients differing by T-stage and confirmed our preclinical observations of MSLN and MMP-9 expression at tumor core level. In the experience of our group and others, MPM local invasion and regional aggressiveness is a major factor preventing surgical resection with curative intent(14, 55); 40% of patients are deemed unresectable on the operating table in spite of extensive pre-operative imaging studies. Based on our observations, we are currently investigating the role of MSLN level in both tumor tissue and patient serum in order to predict resectability for patients with a low clinical 'T' stage based. In addition, recent cancer vaccine clinical trials in patients with pancreatic cancer have demonstrated the beneficial effects of MSLN-specific immune responses in prolonging survival(56, 57) – a feature currently being explored for the development of MSLN-targeted immunotherapies by our group and others(58-60). This study provides further rationale for investigating MSLN-targeted therapies in MPM, as MSLN provides a molecular target that is commonly expressed in human epithelioid MPM and promotes tumor invasion.

In summary, this study is the first to demonstrate an association between MSLN expression and tumor MMP-9 secretion in MPM. We also illustrate the association

between MSLN expression and local tumor invasion in MPM. These results are consistent with the fact that MSLN-expressing solid tumors such as MPM, pancreatic cancer and serous ovarian carcinoma uniformly display regionally aggressive features and dismal outcomes. We have demonstrated our findings not only *in vitro*, but also *in vivo*. The strength of these observations is highlighted by the use of a clinically relevant orthotopic mouse model, which accurately recapitulates human disease and provides an appropriate pleural tumor microenvironment to investigate tumor cell invasion and MSLN biology. Our observations are reproduced with both human and murine MSLN cells and have been verified in samples from 139 human epithelioid MPM tumors. This study provides a better understanding of the locoregional aggressiveness of MSLN-expressing tumors, demonstrates MSLN's impact on tumor MMP, and provides rationale for further clinical study of MSLN as a potential therapeutic target.

Acknowledgements

We thank Drs. William Travis and Kyuichi Kadota for pathologic review and interpretation of human specimens and Irina Linkov for immunohistochemistry.

Grant Support

This work was supported in part by PR101053 Department of Defense Research Grant; Mesothelioma Applied Research Foundation (MARF) Grant in memory of Lance S. Ruble; William H. Goodwin and Alice Goodwin, the Commonwealth Foundation for Cancer Research, the Experimental Therapeutics Center of Memorial Sloan-Kettering Cancer Center; American Association for Thoracic Surgery (AATS)-Third Edward D. Churchill Research Scholarship; IASLC – International Association for the Study of Lung Cancer Young Investigator Award; National Lung Cancer Partnership/LUNGevity Foundation Research Grant; Stony Wold-Herbert Fund, New York State Empire Clinical Research Investigator Program (ECRIP); and U54CA137788/U54CA132378 from the National Cancer Institute.

References

1. Hassan R, Bera T, Pastan I. Mesothelin: a new target for immunotherapy. Clin Cancer Res. 2004;10:3937-42.
2. Ho M, Bera TK, Willingham MC, Onda M, Hassan R, FitzGerald D, et al. Mesothelin expression in human lung cancer. Clinical cancer research : an official journal of the American Association for Cancer Research. 2007;13:1571-5.
3. Hassan R, Ho M. Mesothelin targeted cancer immunotherapy. Eur J Cancer. 2008;44:46-53.
4. Cristaudo A, Foddis R, Vivaldi A, Guglielmi G, Dipalma N, Filiberti R, et al. Clinical significance of serum mesothelin in patients with mesothelioma and lung cancer. Clin Cancer Res. 2007;13:5076-81.
5. Grigoriu BD, Scherpereel A, Devos P, Chahine B, Letourneux M, Lebailly P, et al. Utility of osteopontin and serum mesothelin in malignant pleural mesothelioma diagnosis and prognosis assessment. Clin Cancer Res. 2007;13:2928-35.
6. Pass HI, Wali A, Tang N, Ivanova A, Ivanov S, Harbut M, et al. Soluble mesothelin-related peptide level elevation in mesothelioma serum and pleural effusions. The Annals of thoracic surgery. 2008;85:265-72; discussion 72.
7. Rai AJ, Flores RM, Mathew A, Gonzalez-Espinoza R, Bott M, Ladanyi M, et al. Soluble mesothelin related peptides (SMRP) and osteopontin as protein biomarkers for malignant mesothelioma: analytical validation of ELISA based assays and characterization at mRNA and protein levels. Clin Chem Lab Med. 2010;48:271-8.
8. Wheatley-Price P, Yang B, Patsios D, Patel D, Ma C, Xu W, et al. Soluble mesothelin-related Peptide and osteopontin as markers of response in malignant mesothelioma. J Clin Oncol. 2010;28:3316-22.
9. Creaney J, Francis RJ, Dick IM, Musk AW, Robinson BW, Byrne MJ, et al. Serum soluble mesothelin concentrations in malignant pleural mesothelioma: relationship to tumor volume, clinical stage and changes in tumor burden. Clin Cancer Res. 2011;17:1181-9.
10. Flores RM, Akhurst T, Gonen M, Zakowski M, Dycoco J, Larson SM, et al. Positron emission tomography predicts survival in malignant pleural mesothelioma. J Thorac Cardiovasc Surg. 2006;132:763-8.
11. Flores RM, Riedel E, Donington JS, Alago W, Ihekweazu U, Krug L, et al. Frequency of use and predictors of cancer-directed surgery in the management of malignant pleural mesothelioma in a community-based (Surveillance, Epidemiology, and End Results [SEER]) population. Journal of thoracic oncology : official publication of the International Association for the Study of Lung Cancer. 2010;5:1649-54.
12. Kadota K, Suzuki K, Sima CS, Rusch VW, Adusumilli PS, Travis WD. Pleomorphic Epithelioid Diffuse Malignant Pleural Mesothelioma. A Clinicopathological Review and Conceptual Proposal to Reclassify as Biphasic or Sarcomatoid Mesothelioma. J Thorac Oncol. 2011;6:In press.
13. Rusch VW, Venkatraman E. The importance of surgical staging in the treatment of malignant pleural mesothelioma. The Journal of thoracic and cardiovascular surgery. 1996;111:815-25; discussion 25-6.

14. Flores RM, Zakowski M, Venkatraman E, Krug L, Rosenzweig K, Dycoco J, et al. Prognostic factors in the treatment of malignant pleural mesothelioma at a large tertiary referral center. J Thorac Oncol. 2007;2:957-65.
15. Richards WG, Godleski JJ, Yeap BY, Corson JM, Chirieac LR, Zellos L, et al. Proposed adjustments to pathologic staging of epithelial malignant pleural mesothelioma based on analysis of 354 cases. Cancer. 2010;116:1510-7.
16. Doi T, Maniwa Y, Tanaka Y, Tane S, Hashimoto S, Ohno Y, et al. MT1-MMP plays an important role in an invasive activity of malignant pleural mesothelioma cell. Exp Mol Pathol. 2011;90:91-6.
17. Tan RJ, Fattman CL, Niehouse LM, Tobolewski JM, Hanford LE, Li Q, et al. Matrix metalloproteinases promote inflammation and fibrosis in asbestos-induced lung injury in mice. American Journal of Respiratory Cell and Molecular Biology. 2006;35:289-97.
18. Adusumilli PS, Eisenberg DP, Stiles BM, Chung S, Chan MK, Rusch VW, et al. Intraoperative localization of lymph node metastases with a replication-competent herpes simplex virus. J Thorac Cardiovasc Surg. 2006;132:1179-88.
19. Servais EL, Colovos C, Kachala SS, Adusumilli PS. Pre-clinical mouse models of primary and metastatic pleural cancers of the lung and breast and the use of bioluminescent imaging to monitor pleural tumor burden. Curr Protoc Pharmacol. 2011;Chapter 14:Unit14 21.
20. Stiles BM, Adusumilli PS, Bhargava A, Stanziale SF, Kim TH, Chan MK, et al. Minimally invasive localization of oncolytic herpes simplex viral therapy of metastatic pleural cancer. Cancer Gene Ther. 2006;13:53-64.
21. Servais EL, Suzuki K, Colovos C, Rodriguez L, Sima C, Fleisher M, et al. An in vivo platform for tumor biomarker assessment. PloS one. 2011;6:e26722.
22. Subramanian A, Tamayo P, Mootha VK, Mukherjee S, Ebert BL, Gillette MA, et al. Gene set enrichment analysis: a knowledge-based approach for interpreting genome-wide expression profiles. Proceedings of the National Academy of Sciences of the United States of America. 2005;102:15545-50.
23. Adusumilli PS, Stiles BM, Chan MK, Mullerad M, Eisenberg DP, Ben-Porat L, et al. Imaging and therapy of malignant pleural mesothelioma using replication-competent herpes simplex viruses. J Gene Med. 2006;8:603-15.
24. Servais EL, Colovos C, Bograd AJ, White J, Sadelain M, Adusumilli PS. Animal models and molecular imaging tools to investigate lymph node metastases. J Mol Med (Berl). 2011;89:753-69.
25. Masood R, Kundra A, Zhu S, Xia G, Scalia P, Smith DL, et al. Malignant mesothelioma growth inhibition by agents that target the VEGF and VEGF-C autocrine loops. Int J Cancer. 2003;104:603-10.
26. Kumar-Singh S, Weyler J, Martin MJ, Vermeulen PB, Van Marck E. Angiogenic cytokines in mesothelioma: a study of VEGF, FGF-1 and -2, and TGF beta expression. J Pathol. 1999;189:72-8.
27. Garbow JR, Wang M, Wang Y, Lubet RA, You M. Quantitative monitoring of adenocarcinoma development in rodents by magnetic resonance imaging. Clin Cancer Res. 2008;14:1363-7.
28. Servais EL, Suzuki K, Colovos C, Rodriguez L, Sima C, Fleisher M, et al. An in vivo platform for tumor biomarker assessment. PLoS One. 2011;in review.

29. Roe OD, Creaney J, Lundgren S, Larsson E, Sandeck H, Boffetta P, et al. Mesothelin-related predictive and prognostic factors in malignant mesothelioma: a nested case-control study. Lung Cancer. 2008;61:235-43.
30. Sandeck HP, Roe OD, Kjaerheim K, Willen H, Larsson E. Re-evaluation of histological diagnoses of malignant mesothelioma by immunohistochemistry. Diagn Pathol. 2010;5:47.
31. Kadota K, Suzuki K, Sima CS, Rusch VW, Adusumilli PS, Travis WD. Pleomorphic epithelioid diffuse malignant pleural mesothelioma: a clinicopathological review and conceptual proposal to reclassify as biphasic or sarcomatoid mesothelioma. Journal of thoracic oncology : official publication of the International Association for the Study of Lung Cancer. 2011;6:896-904.
32. Roy DK, O'Neill TW, Finn JD, Lunt M, Silman AJ, Felsenberg D, et al. Determinants of incident vertebral fracture in men and women: results from the European Prospective Osteoporosis Study (EPOS). Osteoporos Int. 2003;14:19-26.
33. Liotta LA, Kohn EC. The microenvironment of the tumour-host interface. Nature. 2001;411:375-9.
34. La Rocca G, Pucci-Minafra I, Marrazzo A, Taormina P, Minafra S. Zymographic detection and clinical correlations of MMP-2 and MMP-9 in breast cancer sera. British journal of cancer. 2004;90:1414-21.
35. Wu ZS, Wu Q, Yang JH, Wang HQ, Ding XD, Yang F, et al. Prognostic significance of MMP-9 and TIMP-1 serum and tissue expression in breast cancer. International journal of cancer Journal international du cancer. 2008;122:2050-6.
36. Jones LE, Humphreys MJ, Campbell F, Neoptolemos JP, Boyd MT. Comprehensive analysis of matrix metalloproteinase and tissue inhibitor expression in pancreatic cancer: increased expression of matrix metalloproteinase-7 predicts poor survival. Clinical cancer research : an official journal of the American Association for Cancer Research. 2004;10:2832-45.
37. Schutz A, Schneidenbach D, Aust G, Tannapfel A, Steinert M, Wittekind C. Differential expression and activity status of MMP-1, MMP-2 and MMP-9 in tumor and stromal cells of squamous cell carcinomas of the lung. Tumour Biol. 2002;23:179-84.
38. Perigny M, Bairati I, Harvey I, Beauchemin M, Harel F, Plante M, et al. Role of immunohistochemical overexpression of matrix metalloproteinases MMP-2 and MMP-11 in the prognosis of death by ovarian cancer. American journal of clinical pathology. 2008;129:226-31.
39. Edwards JG, McLaren J, Jones JL, Waller DA, O'Byrne KJ. Matrix metalloproteinases 2 and 9 (gelatinases A and B) expression in malignant mesothelioma and benign pleura. Br J Cancer. 2003;88:1553-9.
40. Roomi MW, Monterrey JC, Kalinovsky T, Niedzwiecki A, Rath M. Modulation of MMP-2 and MMP-9 by cytokines, mitogens and inhibitors in lung cancer and malignant mesothelioma cell lines. Oncology reports. 2009;22:1283-91.
41. Chang MC, Chen CA, Chen PJ, Chiang YC, Chen YL, Mao TL, et al. Mesothelin Enhances Invasion of Ovarian Cancer by Inducing MMP-7 through MAPK/ERK and JNK Pathways. Biochem J. 2011.
42. Nasu M, Carbone M, Gaudino G, Ly BH, Bertino P, Shimizu D, et al. Ranpirnase Interferes with NF-kappaB Pathway and MMP9 Activity, Inhibiting Malignant Mesothelioma Cell Invasiveness and Xenograft Growth. Genes Cancer. 2011;2:576-84.

43. Kan JS, Delassus GS, D'Souza KG, Hoang S, Aurora R, Eliceiri GL. Modulators of cancer cell invasiveness. Journal of cellular biochemistry. 2010;111:791-6.
44. Sakamoto Y, Dai N, Hagiwara Y, Satoh K, Ohashi N, Fukamachi K, et al. Serum level of expressed in renal carcinoma (ERC)/ mesothelin in rats with mesothelial proliferative lesions induced by multi-wall carbon nanotube (MWCNT). J Toxicol Sci. 2010;35:265-70.
45. Liebig B, Brabletz T, Staege MS, Wulfanger J, Riemann D, Burdach S, et al. Forced expression of deltaN-TCF-1B in colon cancer derived cell lines is accompanied by the induction of CEACAM5/6 and mesothelin. Cancer letters. 2005;223:159-67.
46. Joshi MB, Ivanov D, Philippova M, Erne P, Resink TJ. Integrin-linked kinase is an essential mediator for T-cadherin-dependent signaling via Akt and GSK3beta in endothelial cells. The FASEB journal : official publication of the Federation of American Societies for Experimental Biology. 2007;21:3083-95.
47. Philippova M, Ivanov D, Joshi MB, Kyriakakis E, Rupp K, Afonyushkin T, et al. Identification of proteins associating with glycosylphosphatidylinositol- anchored T-cadherin on the surface of vascular endothelial cells: role for Grp78/BiP in T-cadherin-dependent cell survival. Mol Cell Biol. 2008;28:4004-17.
48. Barth TF, Bruderlein S, Rinaldi N, Mechtersheimer G, Moller P. Pleural mesothelioma mimics the integrin profile of activated, sessile rather than detached mesothelial cells. International journal of cancer Journal international du cancer. 1997;72:77-86.
49. Daemi N, Thomasset N, Lissitzky JC, Dumortier J, Jacquier MF, Pourreyron C, et al. Anti-beta4 integrin antibodies enhance migratory and invasive abilities of human colon adenocarcinoma cells and their MMP-2 expression. International journal of cancer Journal international du cancer. 2000;85:850-6.
50. Gubbels JA, Belisle J, Onda M, Rancourt C, Migneault M, Ho M, et al. Mesothelin-MUC16 binding is a high affinity, N-glycan dependent interaction that facilitates peritoneal metastasis of ovarian tumors. Molecular cancer. 2006;5:50.
51. Uehara N, Matsuoka Y, Tsubura A. Mesothelin promotes anchorage-independent growth and prevents anoikis via extracellular signal-regulated kinase signaling pathway in human breast cancer cells. Mol Cancer Res. 2008;6:186-93.
52. Chang MC, Chen CA, Hsieh CY, Lee CN, Su YN, Hu YH, et al. Mesothelin inhibits paclitaxel-induced apoptosis through the PI3K pathway. Biochem J. 2009;424:449-58.
53. Prieve MG, Moon RT. Stromelysin-1 and mesothelin are differentially regulated by Wnt-5a and Wnt-1 in C57mg mouse mammary epithelial cells. BMC Dev Biol. 2003;3:2.
54. Fukamachi K, Tanaka H, Hagiwara Y, Ohara H, Joh T, Iigo M, et al. An animal model of preclinical diagnosis of pancreatic ductal adenocarcinomas. Biochem Biophys Res Commun. 2009;390:636-41.
55. Rice DC, Erasmus JJ, Stevens CW, Vaporciyan AA, Wu JS, Tsao AS, et al. Extended surgical staging for potentially resectable malignant pleural mesothelioma. Ann Thorac Surg. 2005;80:1988-92; discussion 92-3.
56. Johnston FM, Tan MC, Tan BR, Jr., Porembka MR, Brunt EM, Linehan DC, et al. Circulating mesothelin protein and cellular antimesothelin immunity in patients with

pancreatic cancer. Clinical cancer research : an official journal of the American Association for Cancer Research. 2009;15:6511-8.

57. Lutz E, Yeo CJ, Lillemoe KD, Biedrzycki B, Kobrin B, Herman J, et al. A lethally irradiated allogeneic granulocyte-macrophage colony stimulating factor-secreting tumor vaccine for pancreatic adenocarcinoma. A Phase II trial of safety, efficacy, and immune activation. Annals of surgery. 2011;253:328-35.

58. Carpenito C, Milone MC, Hassan R, Simonet JC, Lakhal M, Suhoski MM, et al. Control of large, established tumor xenografts with genetically retargeted human T cells containing CD28 and CD137 domains. Proceedings of the National Academy of Sciences of the United States of America. 2009;106:3360-5.

59. Hassan R, Ebel W, Routhier EL, Patel R, Kline JB, Zhang J, et al. Preclinical evaluation of MORAb-009, a chimeric antibody targeting tumor-associated mesothelin. Cancer Immun. 2007;7:20.

60. Hassan R, Lerner MR, Benbrook D, Lightfoot SA, Brackett DJ, Wang QC, et al. Antitumor activity of SS(dsFv)PE38 and SS1(dsFv)PE38, recombinant antimesothelin immunotoxins against human gynecologic cancers grown in organotypic culture in vitro. Clinical cancer research : an official journal of the American Association for Cancer Research. 2002;8:3520-6.

Figure Legends

Figure 1. MSLN expression promotes invasion and migration *in vitro* without affecting proliferation. (**A**) Flow cytometry histogram showing MSTO-211H mesothelioma cells transduced with human MSLN by use of retroviral vector to stably overexpress MSLN (dark shading) compared to isotype control (light shading). (**B**) Flow cytometric analysis of murine MSLN expression in AB12 (dark shading), AB12shRNA (dotted line), and isotype control (light shading). (**C**) Cell counting assay demonstrates equivalent cell proliferation *in vitro* comparing MSTO-211H MSLN-positive and MSLN- negative MPM cells. (**D**) Cellular migration and invasion of MSTO-211H was determined by plating equivalent cell number of MSLN-positive or negative MPM cells in standardized transwell Boyden chambers. (**E**) MSLN expression significantly increased both cell migration and invasion *in vitro* ($p<0.001$) in MSTO-211H (left panel). Migration and invasion of AB12 cells (right panel) with naturally expressing MSLN (AB12) and MSLN-knockdown (AB12shRNA) demonstrates a correlation between increased MSLN-expression and increased migration and invasion ($p<0.001$).

Figure 2. Characterization of a clinically relevant orthotopic mouse model of MPM for investigating MSLN biology. (**A**) MPM tumor in the orthotopic mouse model resembles human disease grossly (top panel) and by MRI (lower panel) as tumor growing along pleural surface and encasing mediastinal structures. In this mouse model: (**B**) Histologically, tumor is distributed along visceral pleural surfaces (left panel, arrowhead), the interlobar fissures (right panel, arrowhead), and parietal pleural surfaces with frequent chest wall invasion (bottom panel, arrow). (**C**) MPM metastases

to mediastinal lymph nodes (circle) confirmed by H&E (top right) and MSLN IHC staining (bottom right). (**D**) Engrafted tumors maintain characteristic IHC tumor markers for MPM even in advanced stages (TTF-1^{-}; WT-1^{+}, Calretinin^{+}, Mesothelin^{+}). (**E**) Immunofluorescence (LYVE-1 (red) – lymphatics; CD34 (green)– vascular endothelium) demonstrates lymphangiogenesis throughout pleural tumor nodules (arrow shows chest wall, arrowhead tumor nodule) with intratumoral vessels (inset).

Figure 3. Validation of bioluminescence imaging (BLI) in the mouse model to quantitatively monitor MSLN effect on tumor burden and progression. (**A**) Flow cytometry dot plots showing human MPM cells (MSTO-211H) stably transduced to express GFP-Luciferase fusion gene (x-axis) in both MSLN-negative (left plot) and positive (right plot) cells. (**B**) *In vitro* validation of BLI shows that BLI signal correlates with cell number over a wide range for both MSLN-negative (r=0.99, p<0.0001) and MSLN-positive (r=0.99, p<0.0001) cells. (**C**) *In vivo* BLI validation by correlating BLI signal (left column) to tumor volume by MRI volume averaging (right column) in mice with orthotopic MPM tumors. (**D**) BLI signal correlated strongly with tumor volume over a wide range of tumor progression in mice with pleural mesothelioma with and without MSLN expression.

Figure 4. Mesothelin expression promotes tumor invasion *in vivo* and decreases survival without affecting tumor proliferation. (**A**) BLI monitors tumor proliferation in mice with orthotopic MPM and reveals no difference in tumor progression between MSLN-positive (n=12, red line) and negative (n=12, blue line) tumors. (**B**) Kaplan-Meier

survival analysis demonstrated mice with MSLN-positive tumors (n=12, red line) have decreased survival compared to MSLN-negative (n=12, blue line) tumors (29 vs. 37 days, *p*=0.001). Results confirmed on multiple repeat experiments. (**C**) Heterogeneous MSLN-expressing MPM tumors in mice show increased MSLN staining at the advancing tumor edge in tumor nodules on both diaphragm (upper image asterisk) and chest wall (lower image arrowhead) (**D**) Mice engrafted with tumors of heterogeneous MSLN expression (arrowhead shows area of absent MSLN expression, asterisk shows area of heterogeneous MSLN expression) demonstrate consistent MSLN positivity at areas of local tumor invasion (upper image arrow). MMP-9 IHC shows increased MMP-9 expression at the leading invasive edge (lower image arrow) compared to baseline MMP-9 expression in the areas of tumor with low levels of MSLN expression (lower image asterisk).

Figure 5. MSLN expression upregulates tumor cell MMP secretion. (**A**) Human MPM cells (MSTO-211H) with and without MSLN expression were compared *in vitro* for MMP secretion by multiplex bead array assay of cell culture supernatant. MMP-1, 2, 7, and 9 were all significantly increased with MSLN expression. (**B**) MSLN knockdown correlated with decreased tumor cell secretion of MMP-9 as determined by multiplex bead assay (* $p<0.01$) in AB12 MPM cells.

Figure 6. Tissue Microarray (TMA) constructed from 139 epithelioid MPM tumors reveals an association between MSLN expression and MMP-9 overexpression. (**A**) Representative TMA cores depicting strong or low MSLN and MMP-9 expression (bar =

50μm). (**B**) MMP-9 expression increases as the proportion of tumor cores showing strong (black) and moderate (grey) expression of MSLN increases as compared to weak (hatched) or absent (white) MSLN expression (p <0.001). (**C**) In patients with invasion into the endothoracic fascia, mediastinal fat, chest wall or pericardium (T3-tumors) there is a trend towards increased strong MSLN expression (black; score 4-5) compared to absent-moderate expression (grey; score 0-3) when compared to T-2 tumors (p=0.05).

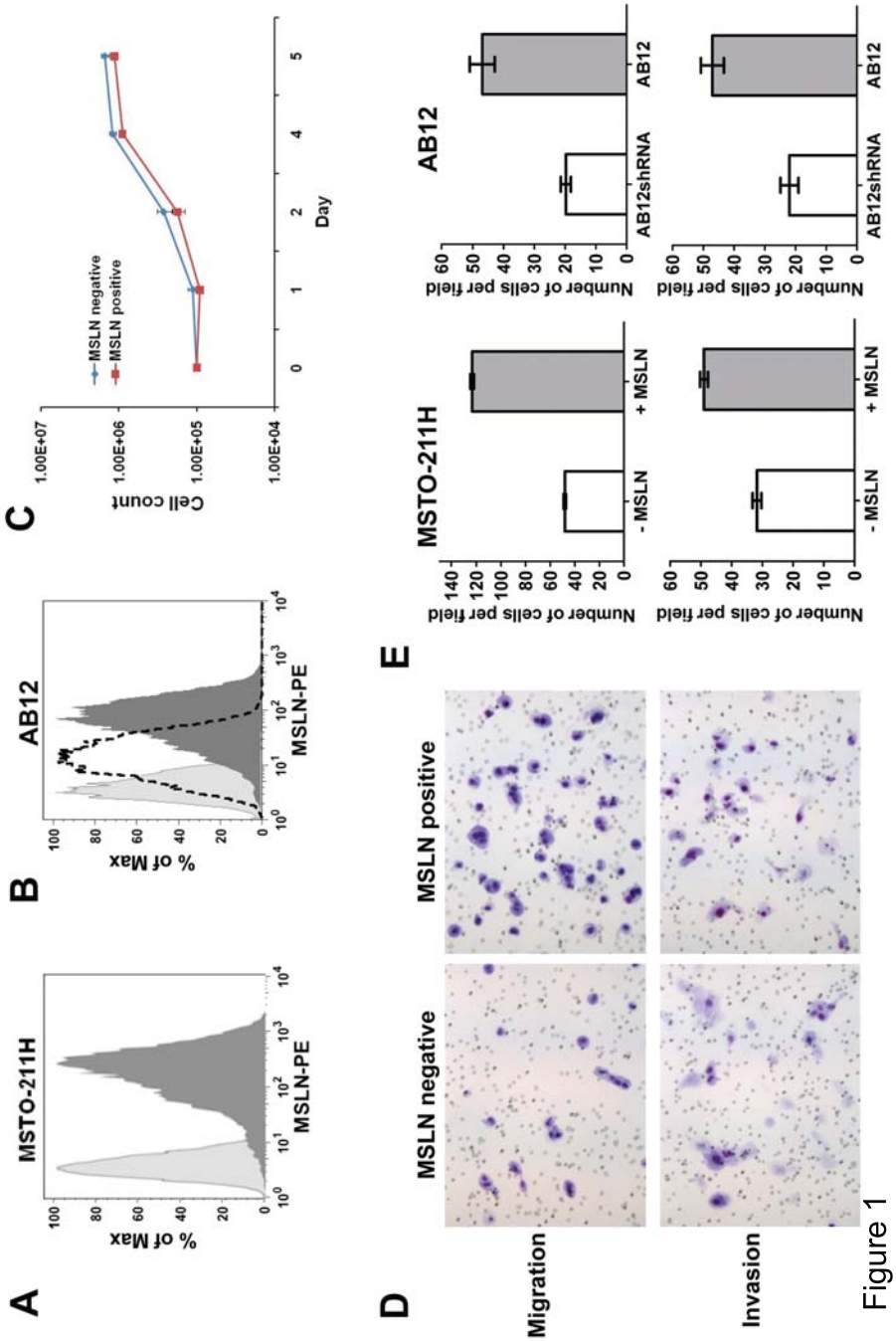

Figure 1

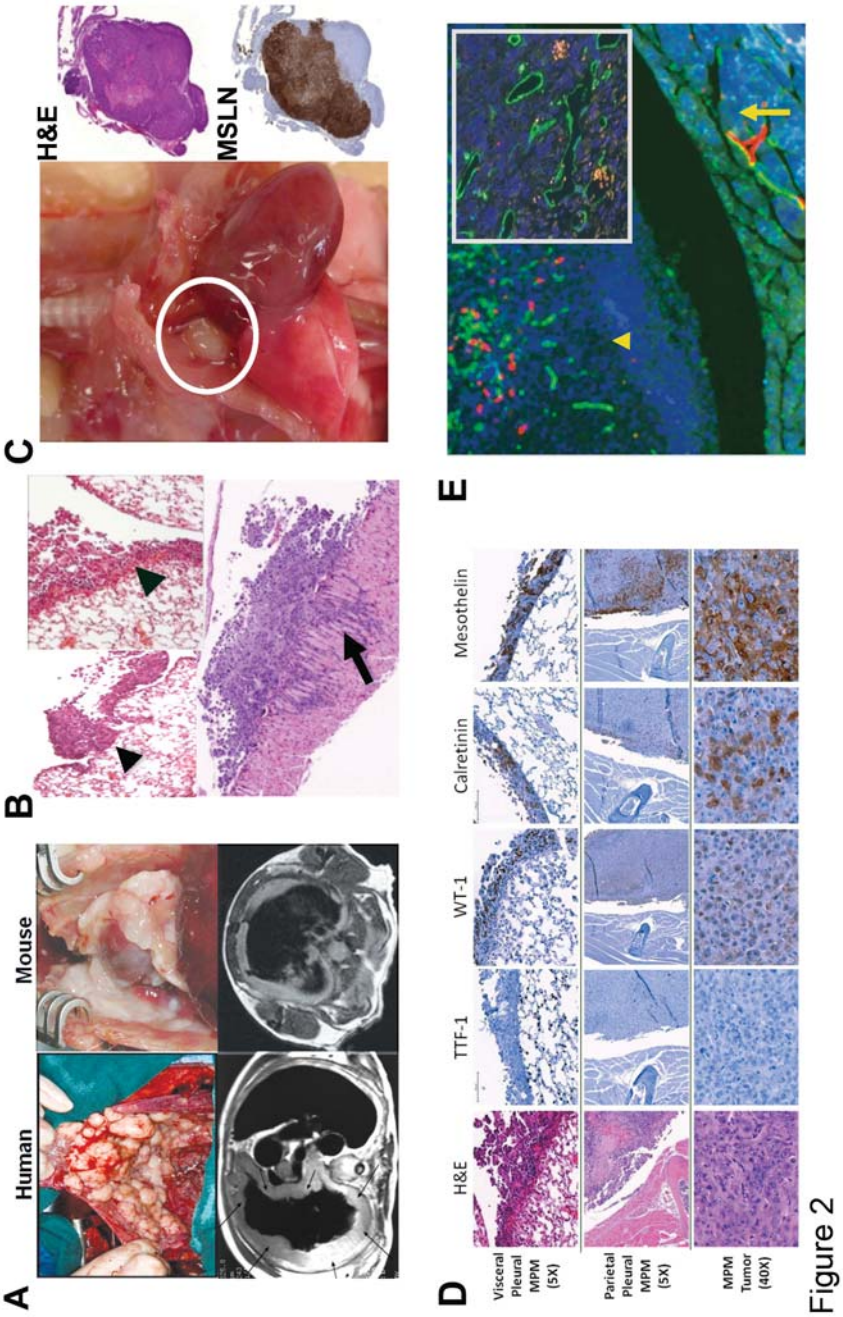

Figure 2

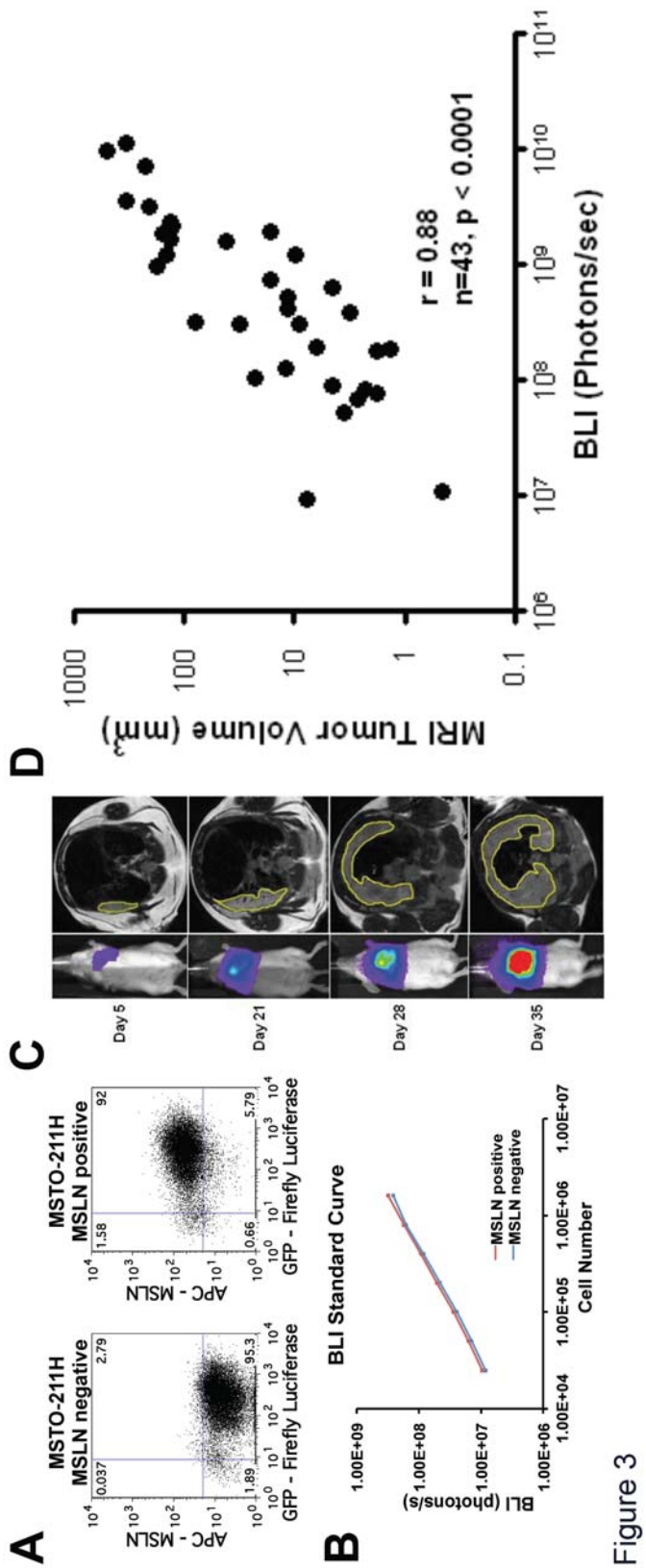

Figure 3

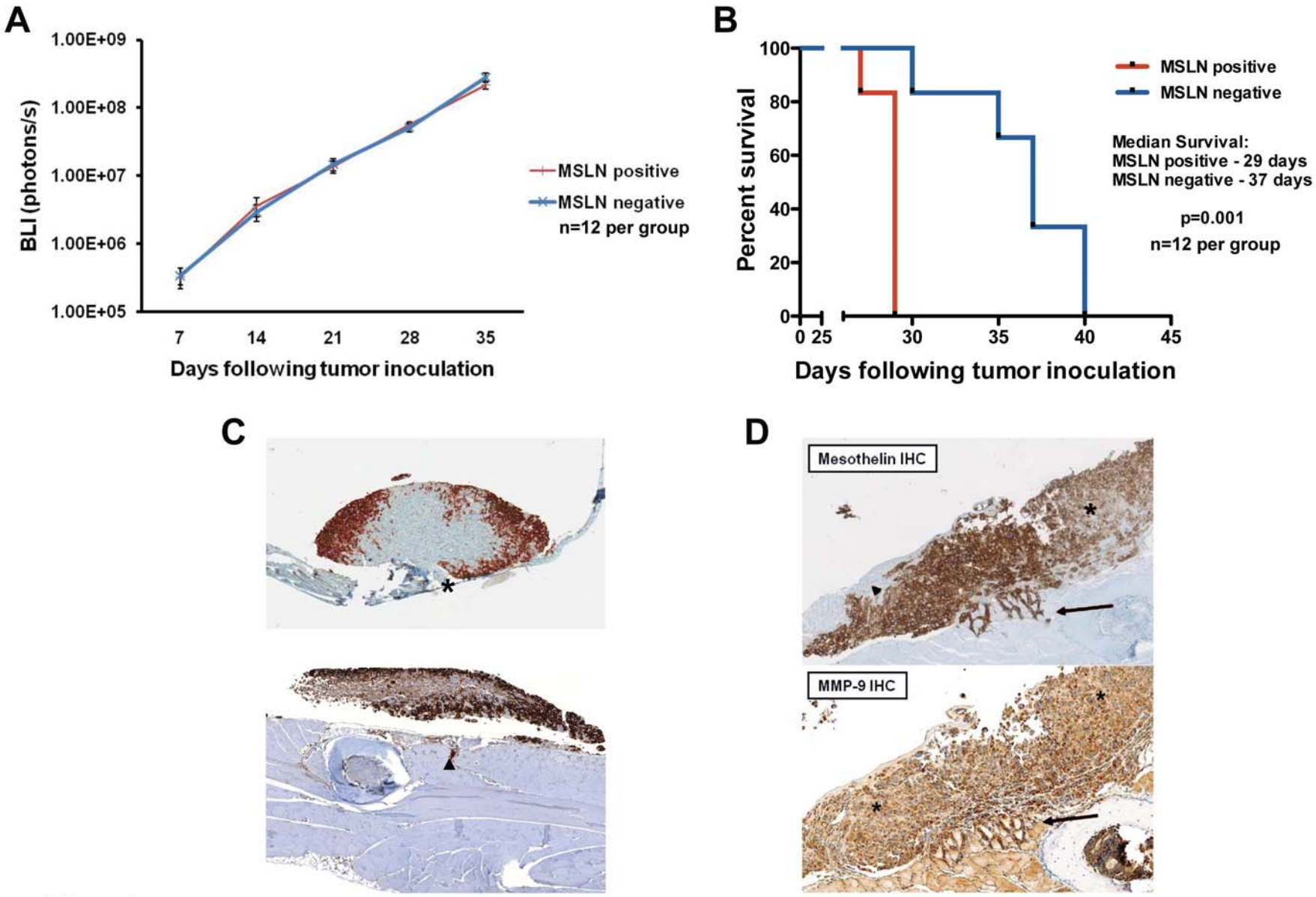

Figure 4

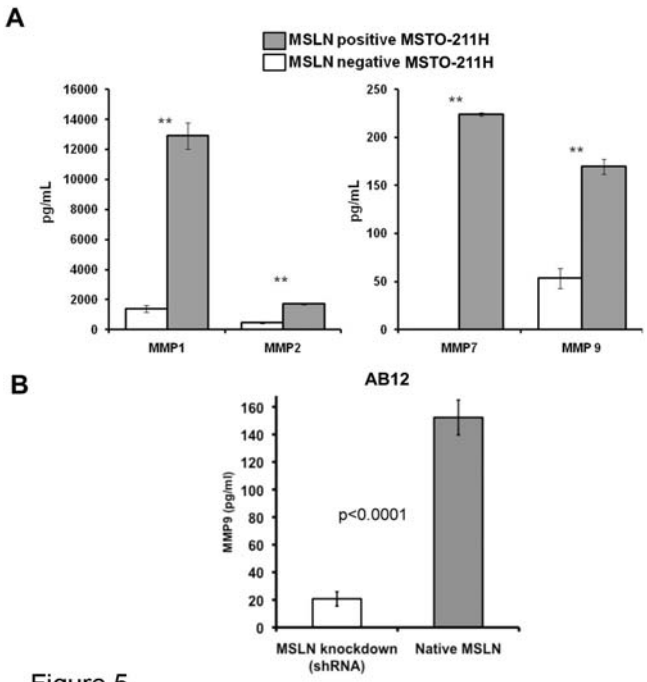

Figure 5

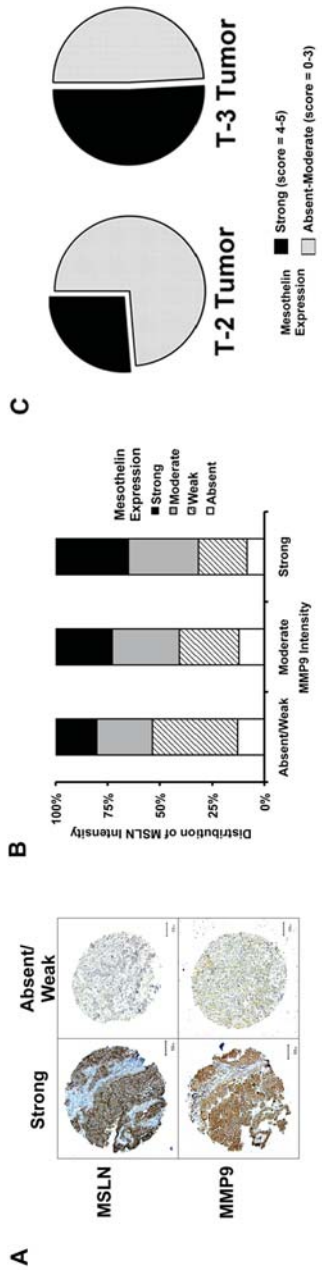

Figure 6

AACR American Association for Cancer Research

Clinical Cancer Research

Mesothelin overexpression promotes mesothelioma cell invasion and MMP-9 secretion in an orthotopic mouse model and in epithelioid pleural mesothelioma patients

Elliot L. Servais, Christos Colovos, Luis A. Rodriguez, et al.

Clin Cancer Res Published OnlineFirst February 27, 2012.